Chem. Mater. **2005,** *17,* 1063−1071

Synthesis and Optical Properties of New End-Functionalized Polyquinolines

S. P. Economopoulos,[†,‡] A. K. Andreopoulou,[†,‡] V. G. Gregoriou,[‡] and J. K. Kallitsis*[,†,‡]

Department of Chemistry, University of Patras, Patras, 26500, Greece, and Foundation for Research and Technology−Hellas, Institute of Chemical Engineering and High-Temperature Processes (FORTH−ICE/HT), Patras 26500, Greece

Received December 1, 2004

A novel monomer incorporating the quinoline moiety as the side group was synthesized and polymerized by employing free radical as well as atom-transfer radical polymerization (ATRP) techniques. In the latter case, two different initiators were used, resulting in dibenzyloxy- or dimethylester-end-functionalized polyquinolines. All polymers were characterized primarily using ^{1}H NMR, gel permeation chromatography, UV−vis photoluminescence spectroscopy, and cyclic voltammetry. A systematic luminescence study was performed in different solvents and concentrations, showing that the optical properties of the newly synthesized polymers depend on both the solution's concentration and the ionic strength of the solvent. In addition, atomic force microscopy and scanning electron microscopy techniques also confirmed the close correlation between the film morphology and the solvent used for their preparation.

Introduction

Material science is focusing more and more toward the development of complex and architectural systems, possessing properties that arise from their detailed structure. The evolution of areas such as photonics and photovoltaics[1,2] strongly depends on the preparation of well-defined, nonconventional materials or the ideal combination of already existing ones, not in a traditional sense, but in ways that will produce new systems. Especially in applications such as polymeric light-emitting diodes (PLEDs) and plastic solar cells where more than one polymeric substances are necessary, but at the same time the blending of many is not always preferred due to miscibility reasons (e.g. thermodynamically), the design and preparation of polymers that bear, in a single chain, all the required functionalities are most preferable.

In these two growing fields, the incorporation of heteroatom-bearing moieties is claimed to be one of the most promising pathways since it brings out properties not easily found in all-carbon structures. One of the most well-established units of this kind is quinolines, which since their incorporation into polymers by Stille and co-workers[3−9] have attracted increased scientific attention due to their ease of synthesis[10] and excellent thermal and mechanical properties, but more importantly due to their interesting photonic, electronic, and conductive properties.[11−18] Further enrichment of their potential use in various applications came from experiments conducted by Jenekhe and Chen, concerning the observed self-assembly of diblock[19,20] and triblock[21] polyquinoline−polystyrene copolymers. Until now, polyquinolines and their copolymers have been successfully used in PLEDs,[22−24] where they have been known to possess excellent electron transporting properties, organic photovoltaic devices[25,26] and selective chemosensors.[27] Moreover, these polymers can be pH-responsive due to the protonation of the imino group,[28,29] thus opening new uses as tunable

---

* Corresponding author. E-mail address. j.kallitsis@chemistry.upatras.gr.

[†] University of Patras.

[‡] Institute of Chemical Engineering and High-Temperature Processes (FORTH−ICE/HT).

(1) *Semiconducting Polymers*; Hadziioannou G., van Hutten P. F., Eds.; Wiley-VCH: Weinheim, Germany, 1999.
(2) Friend, R. H.; Gymer, R. W.; Holmes, A. B.; Burroughes, J. H.; Marks, R. N.; Taliani, C.; Bradley, D. D. C. B.; Dos Santos, D. A.; Brédas, J. L.; Lögdlund, M.; Salaneck, W. R. *Nature* **1999**, *39*7, 121, and references therein.
(3) Wolfe, J. F.; Stille, J. K. *Macromolecules* **1976**, *9*, 489.
(4) Norris, S. O.; Stille, J. K. *Macromolecules* **1976**, *9*, 496.
(5) Wrasidlo, W.; Stille, J. K. *Macromolecules* **1976**, *9*, 505.
(6) Wrasidlo, W.; Norris, S. O.; Wolfe, J. F.; Katto, T.; Stille, J. K. *Macromolecules* **1976**, *9*, 512.
(7) Beever, W. H.; Stille, J. K. *Macromolecules* **1979**, *12*, 1033.
(8) Stille, J. K.; Harris, R. M.; Padaki, S. M. *Macromolecules* **1981**, *14*, 486.
(9) Sybert, P. D.; Beever, W. H.; Stille, J. K. *Macromolecules* **1981**, *14*, 493.
(10) Friedländer, P. *Chem. Ber.* **1882**, *15*, 2572.
(11) Zimmermann, E. K.; Stille, J. K. *Macromolecules* **1985**, *18*, 321.
(12) Tunney, S. E.; Suenaga, J.; Stille, J. K. *Macromolecules* **1987**, *20*, 258.
(13) Parker, I. D.; Pei, Q.; Marrocco, M. *Appl. Phys. Lett.* **1994**, *65*, 1272.
(14) Jenekhe, S. A.; Zhang, X.; Chen, X. L. *Chem. Mater.* **1997**, *9*, 409.
(15) Zhang, X.; Shetty, A. S.; Jenekhe, S. A. *Macromolecules* **1999**, *32*, 7422.
(16) Abkowitz, M. A.; Antoniadis, H.; Agrawal, A. K.; Jenekhe, S. A. *Solid State Commun.* **1992**, *83*, 937.
(17) Kim, K. A.; Park, S. Y.; Kim, N.; Hong, S. I.; Sasabe, H. *J. Appl. Polym. Sci.* **1992**, *46*, 1.
(18) Agrawal, A. K.; Jenekhe, S. A.; Vanherzeele, H.; Meth, J. S. *J. Phys. Chem.* **1992**, *96*, 2837.
(19) Jenekhe, S. A.; Chen, X. L. *Science* **1998** *279*, 1903.
(20) Jenekhe, S. A.; Chen, X. L. *Science* **1999**, *283*, 372.
(21) Chen, X. L.; Jenekhe, S. A. *Macromolecules* **2000**, *33*, 4610.
(22) Zhang, X.; Jenekhe, S. A. *Macromolecules* **2000**, *33*, 2069.
(23) Hide, F.; Yang, Y.; Heeger, A. J. *Synth. Met.* **1997** *85*, 1355.
(24) Kim, J. L.; Kim, J. K.; Cho, H. N.; Kim, D. Y.; Kim, C. Y.; Hong, S. I. *Macromolecules* **2000**, *33*, 5880.
(25) Alam, M. M.; Jenekhe, S. A. *J. Phys. Chem. B* **2001**, *105*, 2479.
(26) Jenekhe, S. A.; Lu, L.; Alam, M. M. *Macromolecules* **2001**, *34*, 7315.
(27) Tong, H.; Wang, L.; Jing, X.; Wang, F. *Macromolecules* **2002**, *35*, 7169.
(28) Lu, L.; Jenekhe, S. A. *Macromolecules* **2001**, *34*, 6249.

10.1021/cm047909r CCC: $30.25

molecules. However, despite their great progress, polyquinolines exhibit intrinsic drawbacks deriving from the low solubilities of such conjugated polymers. Thus, synthetic efforts are still devoted toward the development of processable polyquinolines.[30−32]

Living and controlled polymerization techniques are appropriate tools in order to obtain polymers and copolymers with precise architectural characteristics, engineered with the properties required for a given application. Among them, atom-transfer radical polymerization[33−35] (ATRP) has proven to be a powerful tool for the construction of a great number of macromolecular systems having a variety in composition, toposelectivity, end-functionalities, and architectures, but at the same time using easily accessible experimental conditions. Moreover, the ATRP route has been shown to tolerate various functionalities in its monomeric parts without disturbing the polymerization reaction. This well-established methodology has been adopted herein for the development of polyquinoline macromolecules having simultaneously the ability to be further incorporated by polymerization or other reactions into more complex macromolecular systems. Designing at first a new vinylquinoline monomer and polymerizing it through ATRP initiated by functional compounds allowed us to produce side-chain polyquinolines decorated at their one end with functional units. This synthetic approach can gain significant interest because of the relative lack of side-chain quinoline monomers in the literature. More importantly, the synthesis of a vinylquinoline monomer can provide a route for the introduction of the quinoline moiety in a number of chemical structures also via copolymerization. One very inspiring possibility would be its polymerization in a "macromonomer" analogous approach with various p-type side-chain end-functionalized polymers aiming at an optimized photovoltaic response. Using a different route, this vinylquinoline can be polymerized using proper, rigid initiators resulting in rod−coil block copolymers containing semiconducting segments, which have been known to produce unique structural motifs.[19,20,36−38]

Experimental Section

Materials and Instrumentation. 2-Amino-5-bromobenzophenone,[9,39] 4-styrylboronic acid (**1**),[40] tetrakis(triphenylpshosphine)-palladium(0) ($Pd(PPh_3)_4$),[41] and the ATRP initiators, 1-((3-(benzyloxy)-5-(bromomethyl)phenoxy)methyl)benzene (**4a**)[42] and 4-[3,5-bis(methoxycarbonyl)phenoxymethyl]benzyl bromide (**4b**),[43] were synthesized according to literature methods. All solvents and reagents were purchased from Aldrich or Merck and used without further purification unless otherwise stated. Dimethylformamide (DMF) was distilled under reduced pressure and stored over molecular sieves. All reactions were performed under argon atmosphere.

Optical absorption spectra were recorded on a Hewlett-Packard 8452A spectrophotometer. Photoluminescence spectra were recorded using a Perkin-Elmer LS45 luminescence spectrometer, by excitation of the sample at the absorption maxima of the UV−vis spectra. Polyquinolines' polymeric films were fabricated either from spin coating or drop casting of dilute solutions (0.2 mg, 10 mL).

^1H NMR spectra were obtained on a Bruker Avance-DPX 400 MHz with deuterated $CHCl_3$ having tetramethylsilane (TMS) as internal standard.

Gel permeation chromatography (GPC) measurements were carried out using a Polymer Lab chromatographer with two Ultra Styragel linear columns (10^4, 500 Å), UV detector (254 nm) polystyrene standards, and $CHCl_3$ as eluent, at 25 °C with a flow rate of 1 mL/min.

Differential scanning calorimetry (DSC) measurements were conducted on a TA Instruments Inc. model DSC Q100 series. The heating and cooling runs were conducted at a rate of 10 °C min^{-1} and were kept constant for all the measurements. Only data from the second heating run were taken into account in order to avoid the effect of thermal history.

Cyclic voltammetry (CV) studies were performed using a standard three-electrode cell. Platinum wires were used as counter and working electrodes. Silver/silver nitrate (0.1 M $AgNO_3$ in acetonitrile) was used as a reference electrode. Tetrabutylammonium hexafluorophosphate ($TBAPF_6$; 98%) from Aldrich was used as electrolyte and was recrystallized three times from acetone and was dried in a vacuum at 100 °C before each experiment. Ferrocene was provided from Aldrich and was purified by sublimation before the experiments. Acetonitrile anhydrous 99.8% CH_3CN was also supplied from Aldrich and was used without further purification. All experiments were carried out in an air-sealed electrochemical cell. Before each experiment the cell was purged with high-purity inert gas for 15 min. Before the start of the measurement the inert gas was turned to "blanket mode". Measurements were recorded using a EG&G Princeton Applied Research potensiostat/galvanostat Model 263A connected to a personal computer running PowerSuite software. The scan rate was kept constant for all CV runs at 100 mV/s.

Atomic force microscopy (AFM) images were obtained using a Topometrix Explorer SPM microscope (Theromicroscopes) equipped with a scanner of maximum ranges of 100 and 10 μm in *xy* and *z* directions, respectively. Scanning electron microscopy (SEM) pictures were taken using a LEO Supra 35VP microscope. The examined thin films of various concentrations (0.1, 0.01 wt %) were fabricated from $CHCl_3$, HCOOH, or THF solutions of polymer **PSDPQ**, filtrated through a Millipore filter of 0.25 μm. A drop of each filtered solution was deposited on a mica substrate and then spin-coated.

Monomer Syntheses. *6-Bromo-2,4-diphenylquinoline (2).* In a round flask under inert atmosphere were added 2-amino-5-bromobenzophenone (5.5 g, 20.0 mmol), acetic acid (10 mL), and H_2SO_4 (98%; 0.1 mL) along with an excess of acetophenone (4.7 mL, 40.0 mmol). The reaction mixture was heated at 110 °C under stirring for 48 h. After cooling, the mixture was slowly added to a

---

(29) Bangcuyo, C. G.; Rampey-Vaughn, M. E.; Quan, L. T.; Michael Angel, S.; Smith, M. D.; Bunz, U. H. F. *Macromolecules* **2002** *35*, 1563.
(30) Pelter, M. W.; Stille, J. K. *Macromolecules* **1990**, *23*, 2418.
(31) Zhu, Y.; Alam, M. M.; Jenekhe, S. A. *Macromolecules* **2002**, *35*, 9844.
(32) Zhu, Y.; Alam, M. M.; Jenekhe, S. A. *Macromolecules* **2003**, *36*, 8958.
(33) Coessens, V.; Pintauer, T.; Matyjaszewski, K. *Prog. Polym. Sci.* **2001**, *26*, 337.
(34) Xia, J.; Matyjaszewski, K. *Chem. Rev.* **2001**, *101*, 2921.
(35) Kamigaito, M.; Ando, T.; Sawamoto, M. *Chem. Rev.* **2001**, *101*, 3689.
(36) Stalmach, U.; de Boer, B.; Videlot, C.; van Huten, P. F.; Hadziioannou, G. *J. Am. Chem. Soc.* **2000**, *122*, 5464.
(37) Tsolakis, P.; Kallitsis, J. K. *Chem. Eur. J.* **2003**, *9*, 936.
(38) Chochos, C. L.; Tsolakis, P.; Gregoriou, V. G.; Kallitsis, J. K. *Macromolecules* **2004**, *37*, 2502.
(39) Davis, R. B.; Pizzini, L. C. *J. Org. Chem.* **1960**, *25*, 1884.
(40) Dondoni, A.; Ghiglione, C.; Marra, A.; Scoponi, M. *J. Org. Chem.* **1998**, *63*, 9535.
(41) (a) Coulson, D. R. *Inorg. Synth.* **1972**, *13*, 121. (b) Tayim, H. A.; Bouldoukian, A.; Awad, F. *J. Inorg. Nucl. Chem* **1970**, *32*, 3799.
(42) Reimann, E. *Chem. Ber.* **1969**, *102*, 2881.
(43) Forier, B.; Dehaen, W. *Tetrahedron* **1999**, *55*, 9829.

Table 1. Reaction Conditions and Molecular Weight Characteristics of the Synthesized Side-Chain Quinoline-Bearing Polymers

polymer	M_n	M_w	PDI
PSDPQi[a]	7 570	14 980	2
PSDPQii[a]	15 260	29 750	1.9
PSDPQiii[a]	40 130	108 750	2.7
PSDPQ-1i[b]	1 460	1 710	1.2
PSDPQ-1ii[c]	15 400	24 640	1.6
PSDPQ-1iii[c]	30 940	54 340	1.8
PSDPQ-2i[b]	1 680	2 040	1.2
PSDPQ-2ii[b]	8 050	11 760	1.5
PSDPQ-2iii[d]	21 040	42 830	2.0

[a] From free radical polymerization. [b] DPE, CuBr, 2,2′-bipyridine. [c] DPE, CuBr, PMDETA; instead of DPE, 5% (m/v) ethylene carbonate was used. [d] DPE, CuBr, PMDETA.

stirred mixture of crushed ice (~40 g) and 25% ammonia solution in water (15 mL). The product was filtrated and washed with hot water and EtOH. The pale yellow product was further purified by refluxing under vigorous stirring in *n*-hexane. Filtration, washing with warm *n*-hexane and subsequent drying under vacuum, afforded 7.0 g of **2**. Yield 95%. ^{1}H NMR (CDCl$_3$): δ 8.19 (d, 2H), 8.10 (d, 1H), 8.09 (s, 1H), 8.03 (d, 1H), 7.83 (s, 1H), 7.78 (dd, 1H), 7.45−7.62 (m, 8H).

2,4-Diphenyl-6-(4-vinylphenyl)quinoline (3). In a carefully degassed three-necked flask were added 6-bromo-2,4-diphenylquinoline (**2**; 2.5 g, 7.0 mmol), 4-styrylboronic acid (**1**; 2.1 g, 14.0 mmol), and Pd(PPh$_3$)$_4$ (0.40 g, 0.35 mmol). To that flask were then added toluene (150 mL) and 2 M Na$_2$CO$_3$ (35 mL). The mixture was heated at 100 °C under vigorous stirring for 48 h. After cooling, the resulted mixture was filtrated and the organic layer was separated, washed with H$_2$O (2 × 50 mL), and evaporated under reduced pressure. The obtained solid was suspended in MeOH and filtrated to afford a pale white solid. Further purification through column chromatography (SiO$_2$) using toluene as eluent afforded 2.2 g of **3**. Yield 82%. M.p. 170 °C. Anal. Calcd for C$_{29}$H$_{21}$N (383): C, 90.86; H, 5.48; N, 3.65. Found: C, 90.6; H, 5.6; N, 3.53. ^{1}H NMR (CDCl$_3$): δ 8.29 (d, 1H), 8.21 (d, 2H), 8.09 (s, 1H), 8.00 (d, 1H), 7.84 (s, 1H), 7.45−7.62 (m, 12H), 6.74 (q, 1H), 5.78 (d, 1H), 5.27 (d, 2H). ^{13}C NMR (CDCl$_3$): δ 156.81, 149.29, 148.30, 139.99, 139.63, 138.57, 138.42, 136.96, 136.29, 130.64, 129.58, 129.37, 128.98, 128.85, 128.71, 128.49, 127.56, 127.49, 126.75, 125.96, 123.19, 119.77, 114.17.

Polymer Syntheses. *Free Radical Polymerization of Vinylquinoline 3.* In a carefully degassed flask the desired ratio of 2,4-diphenyl-6-(4-vinylphenyl)quinoline (**3**) and asobis(isobutyronitrile) (AIBN), and DMF (0.5 mL) were added and the mixture was heated at 80 °C for 24 h. After cooling it was precipitated in MeOH and filtrated to obtain a pale white solid. Any monomer residual in the product was removed through washing with warm ethyl acetate, thus affording the desired polymer **PSDPQ**. Yield 70−85%. Molecular characteristics of the polymers are given in Table 1, entries 1−3 obtained from monomer/AIBN ratios of 30/1 (**PSDPQi**), 75/1 (**PSDPQii**), and 150/1 (**PSDPQiii**), respectively. ^{1}H NMR (CDCl$_3$) δ: 7.1−8.05 (three broad, 16H), 6.4 (broad, 2H), 1.3−2.2 (two broad, 3H).

ATRP Polymerization of Vinylquinoline 3 Using Initiator 4a. A round-bottomed flask equipped with a U-tube, a rubber septum, magnetic stirrer, and a gas inlet/outlet was carefully degassed. Initiator **4a** (0.015 g, 0.039 mmol) was added to the flask containing CuBr (0.011 g, 0.078 mmol) and 2,2′-bipyridine (0.012 g, 0.078 mmol) along with 2,4-diphenyl-6-(4-vinylphenyl)quinoline (**3**; 0.150 g, 0.39 mmol) and diphenyl ether (1.5 mL). The system was degassed three times and filled with argon. The reaction mixture was heated at 110 °C for 24 h. After cooling, 5 mL of CHCl$_3$ was added and the solution was filtrated through a silica column, to remove the catalyst, and precipitated in excess of MeOH. The obtained polymer was dried under vacuum. Any unreacted monomer was removed by washing with warm ethyl acetate. **PSDPQ-1i**: Yield 50%. $M_n = 1460$. $M_w = 1710$ (Table 1, entry 4). ^{1}H NMR (CDCl$_3$): δ 6.4−8.5 (six broad, 31H), 4.92 (broad, 4H), 1.3−2.4 (two broad, 3H).

ATRP Polymerization of Vinylquinoline 3 Using Initiator 4b. A round-bottomed flask equipped with a U-tube, a rubber septum, magnetic stirrer, and a gas inlet/outlet was carefully degassed. Initiator **4b** (0.015 g, 0.038 mmol) was added to the flask containing CuBr (0.011 g, 0.078 mmol) and 2,2′-bipyridine (0.012 g, 0.078 mmol) along with **3** (0.150 g, 0.39 mmol) and diphenyl ether (1.5 mL). The system was degassed three times and filled with argon. The reaction mixture was heated at 110 °C for 24 h. After cooling, 5 mL of CHCl$_3$ was added and the solution was filtrated through

Scheme 1[a]

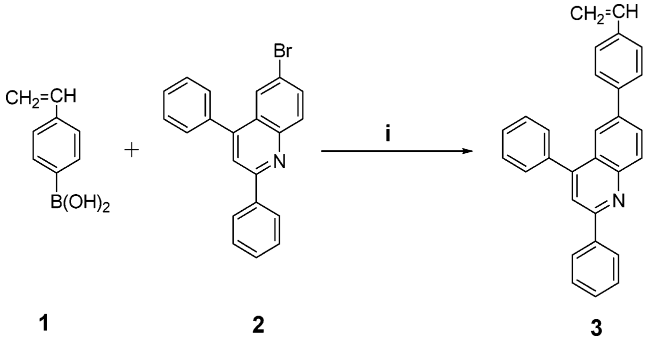

[a] (i) Toluene, Na$_2$CO$_3$ 2 M, Pd(PPh$_3$)$_4$, Reflux for 48 H, 82%.

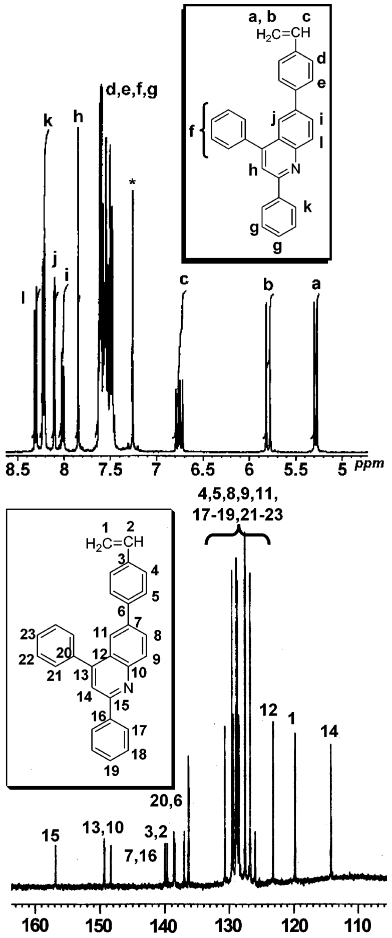

Figure 1. ^{1}H and ^{13}C NMR spectra, of monomer **3** in CDCl$_3$, upper and lower parts, respectively.

Scheme 2. ATRP Polymerization of Monomer 3[a]

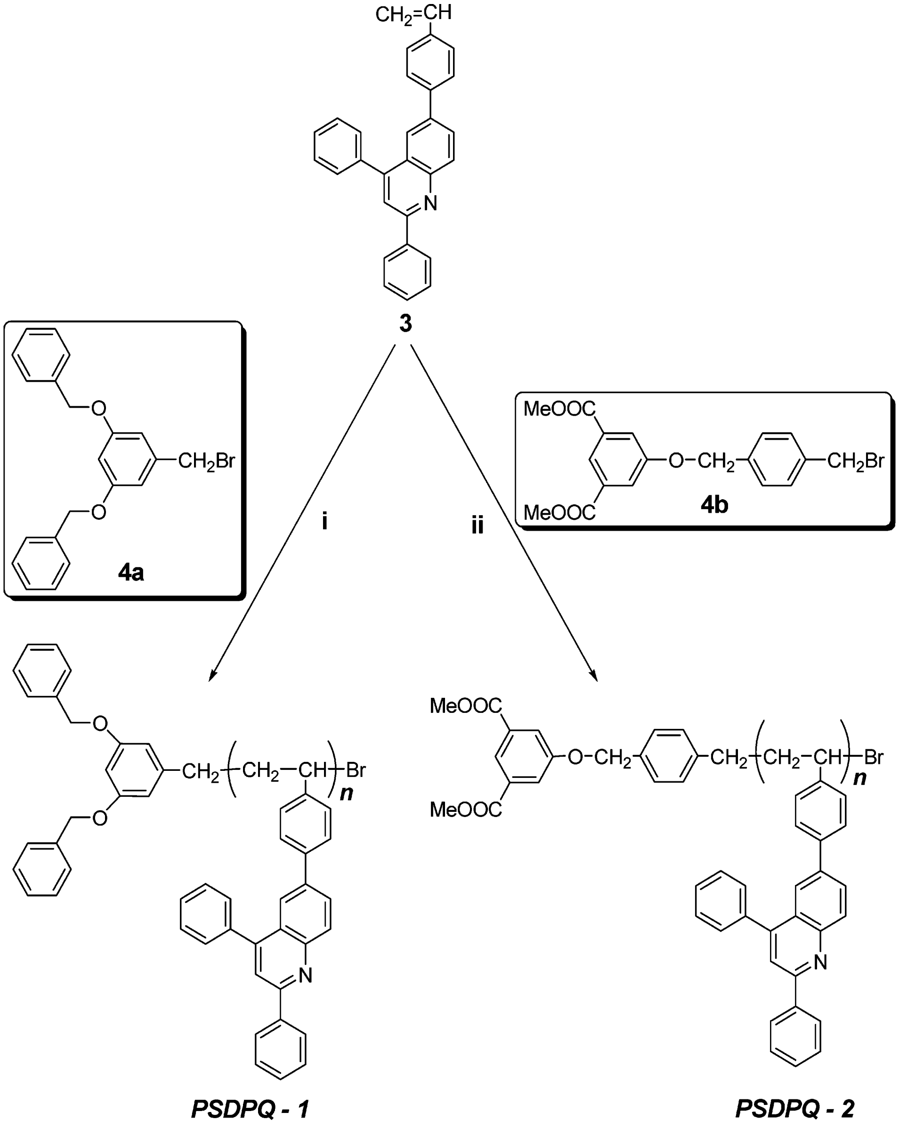

[a] (i) CuBr, 2,2′-bipyridine, diphenyl ether, 110 °C or PMDETA, 5% (m/v) diphenyl ether, ethylene carbonate, 110 °C; (ii) CuBr, 2,2′-bipyridine or PMDETA, diphenyl ether, 110 °C.

a silica column, to remove the catalyst, and precipitated in excess of MeOH. The obtained polymer was dried under vacuum. Any unreacted monomer was removed by washing with warm ethyl acetate. **PSDPQ-2i**: Yield 60%. $M_n = 1680$. $M_w = 2040$ (Table 1, entry 7). ^{1}H NMR (CDCl$_3$): δ 7.0−8.4 (five broad, 25H), 5.1 (broad, 2H), 3.92 (broad, 6H), 1.3−2.3 (two broad, 3H).

Results and Discussion

Syntheses and Characterization. For the preparation of the vinylquinoline monomer **3**, a palladium-mediated Suzuki coupling reaction[44] was performed between the vinylphenylboronic acid (**1**) and 2,4-diphenyl-6-(4-vinylphenyl)quinoline (**2**), Scheme 1. 2,4-Diphenyl-6-(4-vinylphenyl)quinoline was synthesized using a different synthetic procedure than the one described in the literature,[45] affording us higher yields. Thus, we obtained the desired monomer in gram-scale quantities, which was fully characterized using ^{1}H and ^{13}C NMR spectroscopy, Figure 1. Its free radical polymerization using AIBN or BPO as the initiator in DMF solutions produced polymeric materials with a variety of molecular weights and in good yields, with respect to the initial monomer amount (Table 1). Moreover, any unreacted monomer could be easily removed due to its excellent and selective solubility in warm ethyl acetate. However, as expected, the molecular weights of the polymers through this particular technique were not controllable. Thus, ATRP was employed in order to obtain polymers with controllable molecular characteristics and at the same time possessing end-functionalities. Since ATRP has proven to be tolerant in a large number of functional monomers as well as initiators, an attempt was been made here to employ it also for the new vinylquinoline monomer **3** and additionally to extend it by using various functional initiators. For this reason, two difunctional aromatic methylene bromides were selected as initiators (Scheme 2, structures **4a**,**b**, respectively) that in the past have also effectively initiated the polymer-

---

(44) Miyaura, N.; Suzuki, A. *Chem. Rev.* **1995**, *95*, 2457.

(45) (a) Song, S. J.; Cho, S. J.; Park, D. K.; Kwon, T. W.; Jenekhe, S. A. *Tetrahedron Lett.* **2003**, *44*, 255. (b) Miyajiima, S.; Ito, K.; Kashiwagura, I.; Kitamura, C. *Nippon Kagaku Kaishi* **1979**, *11*, 1514.

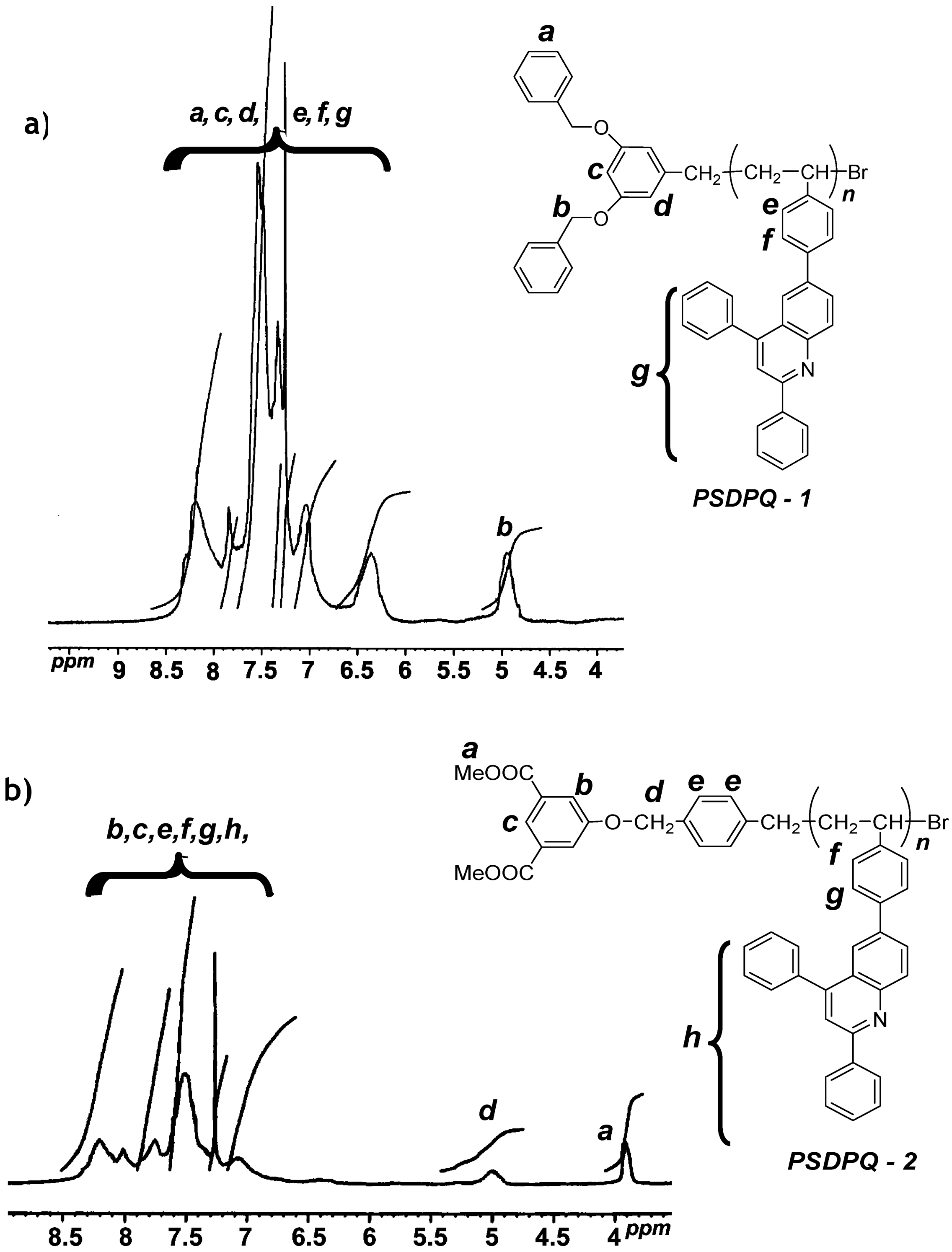

Figure 2. ^{1}H NMR spectra of polymers (a) **PSDPQ-1i** and (b) **PSDPQ-2i** in $CDCl_3$.

ization of styrene.[46] Through this approach we are trying to extend the use of drastic initiators for the polymerization of nontraditional vinylic monomers, a procedure that may prove useful for the polymerization of many other future monomers with various functionalities leading to polymers appropriate for different technological applications.

Different ratios of monomer to initiator with copper bromide (CuBr) as the catalyst and either *N*,*N*,*N*′,*N*′,*N*″-pentamethyldiethylenetriamine (PMDETA) or 2,2′-bipyridine as bases have been used (Scheme 2). In all cases, the reaction time was approximately $t = 1$day in order to achieve higher conversions. In these cases the polydispersity values (PDI) are low only for the low molecular weight samples, while for higher MW, the polymerization control was poor (see Table 1). Nevertheless, the presence of a functional group on the polymer's end and the low polydispersity for the low MW samples enables further use of these systems as macromonomers for incorporation into more complex architectures. The GPC traces of a sample obtained by ATRP

---

[46] Deimede, V.; Kallitsis, J. K. *Chem. Eur. J.* **2002**, *8*, 467.

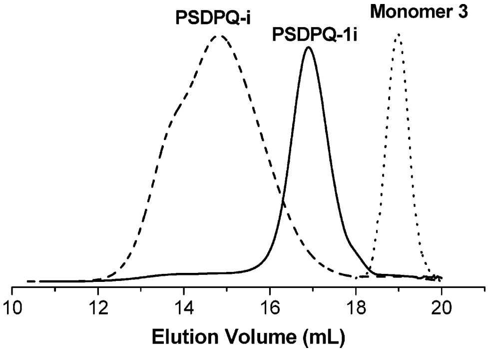

Figure 3. GPC traces of polymers **PSDPQ-I** (free radical polymerization) and **PSDPQ-1i** (ATRP) and of the initial monomer **3**.

are depicted in Figure 3, in comparison with a sample from free radical polymerization, showing the control of the polymerization obtained by the ATRP methodology for the low MW counterparts. Structural evidence for the successful incorporation of the initiators to the polymers can be found at the ^{1}H NMR spectra of the dibenzyloxy initiated polymer (**PSDPQ-1i**) and of the α-dicarboxylic acid methylester initiated one (**PSDPQ-2i**), Figure 2a,b, respectively. For the lower molecular weight analogy, an estimation of the molecular weight can be obtained from the presence of the end groups due to the incorporation of the initiator moiety in every polymer chain as it is assured from the used polymerization technique (ATRP). Thus the calculated MW for the sample **PSDPQ-1i** based on the methylene protons of the initiator and all aromatic protons is equal to 1900, which is in fairly good agreement with the value of 1460 from the GPC results, despite the fact that polystyrene standards were used for calibration. In analogy, the calculation of the MW for **PSDPQ-2i** based on the methyl ester protons was found to be 2300, also in fairly good agreement with the value of 1680 as given in Table 1. The final polymeric materials are soluble in many common organic solvents such as $CHCl_3$, THF, HCOOH, DMA, toluene, and *o*-DCB. By simply removing the end-protective groups (methyl ester or benzyl ones) from the **PSDPQ-1** and **PSDPQ-2** samples, end-functionalized polyquinolines can be obtained, providing the opportunity to be further incorporated into other more complex polymeric architectures.

Examination of the polymers' thermal properties using differential scanning calorimetry (DSC) revealed that these particular polyquinolines are amorphous. For example the **PSDPQ-1iii** sample presented a glass transition temperature (T_g) at 205 °C. This T_g is higher than the value of 185 °C previously reported in the literature for other side-chain polyquinolines[28] and presents an additional advantage, of the polymers reported here, for their future employment in PLEDs or plastic solar cells. When comparing similar molecular weights of the different polymers synthesized, no significant variation in the glass transition temperature can be observed.

Cyclic Voltammetry. All synthesized polymers, as well as the initial monomer **3**, were studied using cyclic voltammetry in an effort to determine their HOMO and LUMO energy levels. The polymers were studied in thin film form, while monomer **3** was studied in 1 mM solution due to its solubility in acetonitrile. The working electrode was cleaned before each experiment through sonication in 65% HNO_3, followed by subsequent sonication in absolute EtOH. The $Ag/AgNO_3$ electrode was connected to the electrochemical cell through a salt bridge and was calibrated before each experiment by running cyclic voltammetry on ferrocene. The potential values obtained versus Ag/Ag^+ were converted versus saturated calomel electrode (SCE). The energy levels were calculated using the following empirical equation:[47-51]

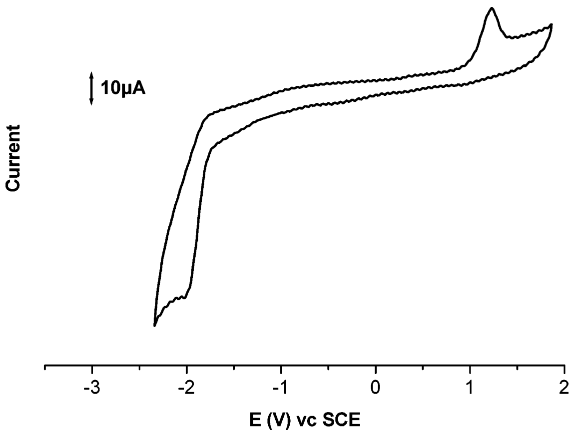

Figure 4. CV of polymer **PSDPQiii** in thin film. Scan rate, 100 mV/s.

$$\mathrm{HOMO} = 4.4 + (E^{\mathrm{ox}}{}_{\mathrm{onset}}) \quad \text{and} \quad \mathrm{LUMO} = 4.4 + (E^{\mathrm{red}}{}_{\mathrm{onset}})$$

Samples were prepared by dipping the working electrode in a viscous 10 wt % chloroform solution of the polymers and subsequent drying. From the cyclic voltammogram in Figure 4, the oxidation peak at 1.2 V with an onset at 1.0 V gives a HOMO energy value of 5.4 eV. The reduction peak at −2.0 (onset −1.9 V) gives a LUMO energy level of 2.5 eV. The electrochemical band gap determined by the oxidation and reduction onsets was calculated at 2.9 eV, which is in fairly good agreement with the optical band gap (as calculated from the onset of the absorption spectra in thin film) of 3.1 eV. Furthermore, the CV of monomer **3** as performed in solution yielded energy levels of 2.6 eV for the LUMO and 5.7 eV for the HOMO. This electrochemical band gap is in good agreement with the calculated optical band gap of 3.1 eV. For this electrochemical experiment, sample **PSDPQiii** was used; however, the electrochemical properties of polymers reported here seem to be unaffected by the polymerization method ATRP− free radical polymerization or by the incorporation of the various initiators.

Optical Properties. Initial monomer **3** and its respective homopolymers were thoroughly examined through absorption and emission spectroscopic techniques. It must be noted that all homopolymers obtained either from free radical or ATRP polymerizations show identical optical characteristics. The absorption-fluorescence spectra of vinyl monomer **3** and of

---

(47) Bredas, J. L.; Silbey, R.; Boudreux, D. S.; Chance, R. R. *J. Am. Chem. Soc.* **1983**, *105*, 6555.

(48) Bredas, J. L. In *Handbook of Conducting Polymers*; Skotheim, T. A., Ed.; Dekker: New York, 1986; pp 859−913.

(49) Bredas, J. L.; Chance, R. R.; Baughman, R. H.; Silbey, R. *J. Chem. Phys.* **1982**, *76*, 3673.

(50) Chance, R. R.; Boudreux, D. S.; Bredas, J. L.; Silbey, R. In *Polymers in Electronics*; Davidson, T., Ed.; ACS Symposium Series 242; American Chemical Society: Washington, DC, 1983; pp 433−446.

(51) Frommer, J. E.; Chance, R. R. *Encyclopedia of Polymer Science and Engineering*, 2nd ed.; Wiley: New York, 1986; Vol. 5, pp 462−507.

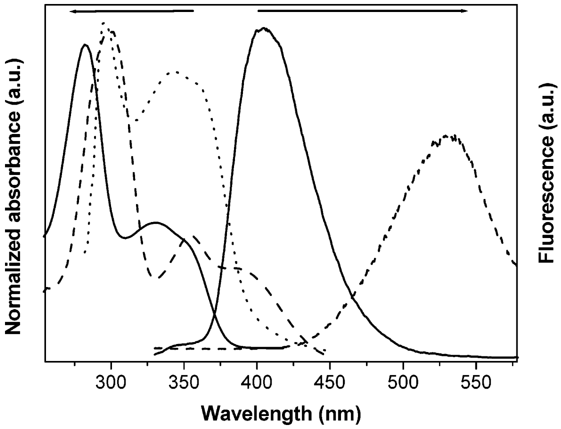

Figure 5. Absorbance spectra of monomer **3** in $CHCl_3$ solution (solid line), in HCOOH solution (dashed line), and in solid state (dotted line). Fluorescence spectra of monomer **3** in $CHCl_3$ solution (solid line) and in HCOOH solution (dashed line).

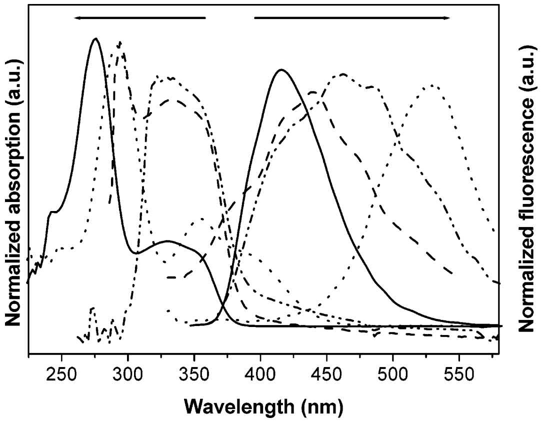

Figure 6. Absorbance of polymer **PSDPQ** in $CHCl_3$ solution (solid line), in HCOOH solution (dotted line), in thin film cast from $CHCl_3$ (dashed line), and in thin film cast from HCOOH (dashed−double-dotted line). Fluorescence spectra of polymer **PSDPQ** in $CHCl_3$ solution (solid line), in HCOOH solution (dotted line), in thin film cast from $CHCl_3$ (dashed line), and in thin film cast from HCOOH (dashed−double-dotted line).

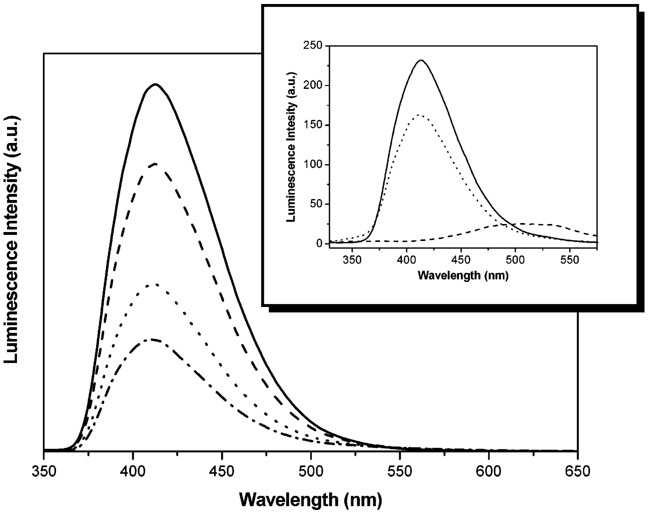

Figure 7. Emission spectra of **PSDPQ** in THF solution (solid line), at a concentration of 0.2 M HCOOH (dashed line), 0.6 M of HCOOH (dotted line), and 1.2 M of HCOOH (dashed−dotted line). Inset: Emission spectra of **PSDPQ** in $CHCl_3$ solution (solid line), at a concentration of 0.4 M of HCOOH (dashed line) and after the addition of NH_3 in the protonated solution (dotted line).

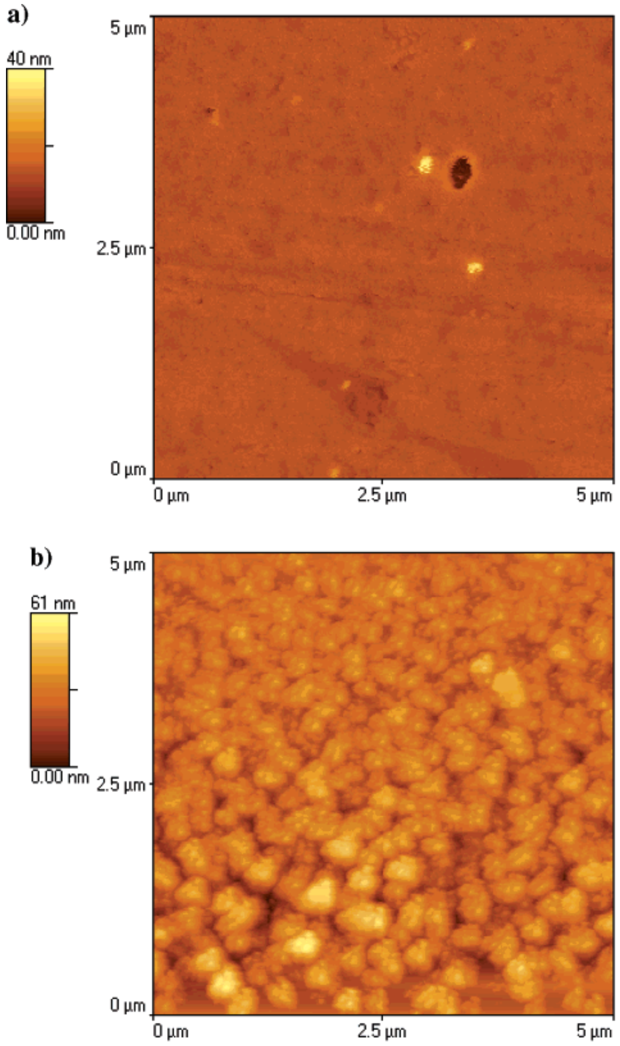

Figure 8. AFM micrographs of surface patterns of polymer **PSDPQ** on mica substrate spin-coated from (a) 0.1 wt % $CHCl_3$ solution and (b) 0.1 wt % HCOOH solution. Each image is a 5 × 5 μm tapping mode AFM scan.

the side-chain quinoline polymer **PSDPQ** in dilute solutions and in thin film form are depicted in Figures 5 and 6, respectively. The $CHCl_3$ solutions exhibit a sharp absorption peak at 282 nm for **3** and at 274 nm for **PSDPQ**, as well as a broader one centered at 332 nm for both cases. The HCOOH solutions show a red shift of the main absorption peak at 300 nm for the monomer and at 293 nm for the polymer, a weaker peak at 355 nm, and a shoulder at around 386 nm (393 nm for **PSDPQ**). Thin films of the monomer or polymer, obtained from either the $CHCl_3$ or the HCOOH solutions present a peak at 295 nm and a broad and more extended one from 330 to 360 nm. The relative intensity of the second peak increases significantly in the solid state compared to its intensity in solution. The high-energy peak is shifted to higher wavelengths both in the solid state and in the acidic solution, an indication for the formation of aggregates probably originating from intra- or intermolecular interactions. This is further supported by the emission spectrum of thin films which is red-shifted compared to the chloroform solution as shown in Figure 6.

In the polymer's case, the main emission peak from the $CHCl_3$ solution appeared at 415 nm compared to 404 nm for the monomer **3** (Figures 6 and 5, respectively). Protonation of both samples using HCOOH as solvent causes a

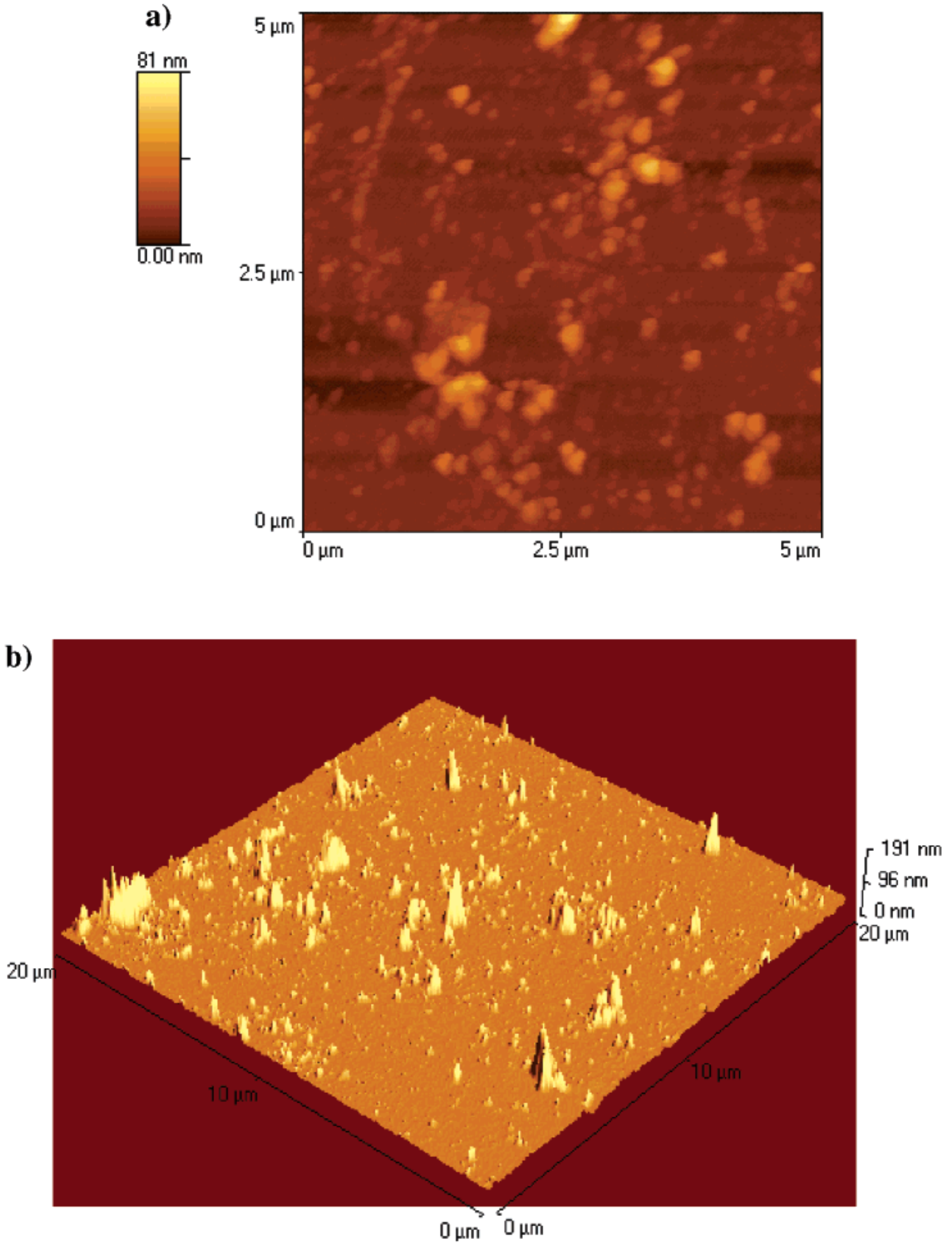

Figure 9. AFM micrographs of polymer **PSDPQ** in its protonated form spin-coated from 0.01 wt % $CHCl_3$ solution: (a) surface pattern 5 × 5 μm and (b) three-dimensional 20 × 20 μm tapping mode AFM scans.

red shift of the emission peak to about 530 nm compared to the observed one in $CHCl_3$ solution. This represents a more than 100 nm red shift, which can be attributed to acid-based interactions of the quinoline group leading to excimer formation. The same phenomenon has been also observed by Lu and Jenekhe for an analogous polymeric material, where interactions of protonated amino groups with neutrally charged ones were suggested as the driving force for the excimer formation.[28] In that report, it was concluded that mostly intramolecular interactions took place on the basis of a comparison of the polymer's behavior to that of a model compound. Since in our case both the **PSDPQ** polymer (Figure 6) and the initial monomer **3** display an analogous red shift when HCOOH is used as the solvent (Figure 5), we can conclude that intermolecular interactions play an additional critical role in our system. To further analyze this behavior, we examined the effect of the solution's concentration on the emission properties where it was proven that for a concentration range of 10^{-4}–10^{-7} M there was no differentiation between the monomer and the polymer, in either of the solvents. In the monomer's case, further decrease of the concentration to 10^{-9} M levels negated the red-shift effect, allowing for a single peak to appear at 455 nm, which is blue-shifted in comparison to the 530 nm peak. This behavior strengthens the notion that intermolecular phenomena are involved in the process and that further dilution of the HCOOH solution weakens the possibility of complex formation, as expected. The influence of the solvent used on the protonation of the **PSDPQ** is presented in Figure 7. In $CHCl_3$ solutions, by addition of a minimal amount of HCOOH, the emission peak at 415 nm is almost quenched, and a weak new peak at 530 nm appears, which is also the case when hydrochloric acid is added in a THF solution. However, when THF was used as solvent, addition of

HCOOH resulted in a more gradual decrease of the emission peak. These differentiations show that the interactions of the protonated species with the polar solvent molecules compete with the interactions between the protonated and nonprotonated species resulting in a more gradual decrease of the peak at 415 nm.

The effect of protonation on the emissive properties of our polymer **PSDPQ** is reversible, as shown in Figure 7 (inset). When formic acid was added to a 10^{-6} M $CHCl_3$ solution of the polymer, the emission peak shifted from 415 to 530 nm. Subsequent addition of ammonia to the same solution forced the peak at 530 nm to disappear and the emission at 415 nm to reappear, in a reversible manner. All the experiments above have shown that under certain conditions this quinoline system possesses sensoring properties against acids in organic media.

Thin Film Morphology. To further understand and analyze the observed differences of the films obtained from $CHCl_3$ and HCOOH solutions, AFM and SEM techniques were employed. In all of the morphology experiments the **PSDPQiii** polymer was used. Thin films spin-coated from 0.1 wt % solution in $CHCl_3$ show the presence of a smooth surface (Figure 8a), while the film casted from 0.1 wt % HCOOH solution shows a completely different morphology, with aggregates in the range of about 300 nm being clearly visible (Figure 8b). A polymeric sample after protonation was isolated and dissolved in $CHCl_3$ or THF. Thin films of 0.01 wt % $CHCl_3$ solution were spin-coated and examined using AFM; see Figure 9, showing some organizational features in a nanometer scale. This organization is much more obvious when the THF solution of the protonated polymers was spin-coated and its film surface was examined with SEM, as shown in Figure 10a,b. Aggregate formation from the THF solution of the protonated **PSDPQ** was unambiguously observed in these images, where homogeneously distributed “islands” in the range of 500 nm are distinguished, supporting the strong tendency of the protonated **PSDPQ** to self-organize into hierarchical structures.

Conclusions

A new quinoline-based monomer has been synthesized and polymerized either using free radical or atom-transfer radical polymerization techniques, resulting in soluble, easily processable, and amorphous polymeric materials. Furthermore, polyquinolines having benzyloxy or methyl ester end groups can be prepared by employing the ATRP technique, by using functional initiators. All polymers were studied with respect to their optical properties. A detailed study of the emission properties both in dilute solutions and in the solid state was performed showing that light-emitting polymers with emissions ranging from 410 to 530 nm were obtained depending on the polymeric structure and the solvent used. Protonation of the polymers resulted in a significant red shift in the range of 100 nm. In addition, the polymers’ thin film morphology as examined by AFM and SEM techniques unambiguously showed the formation of nanoscaled structures, which correlate well to the above-described optical experiments. Additionally, cyclic voltammetry experiments allowed the estimation of the polymers’ energy levels that are in the range of 2.5 and 5.4 eV for the LUMO and HOMO, respectively.

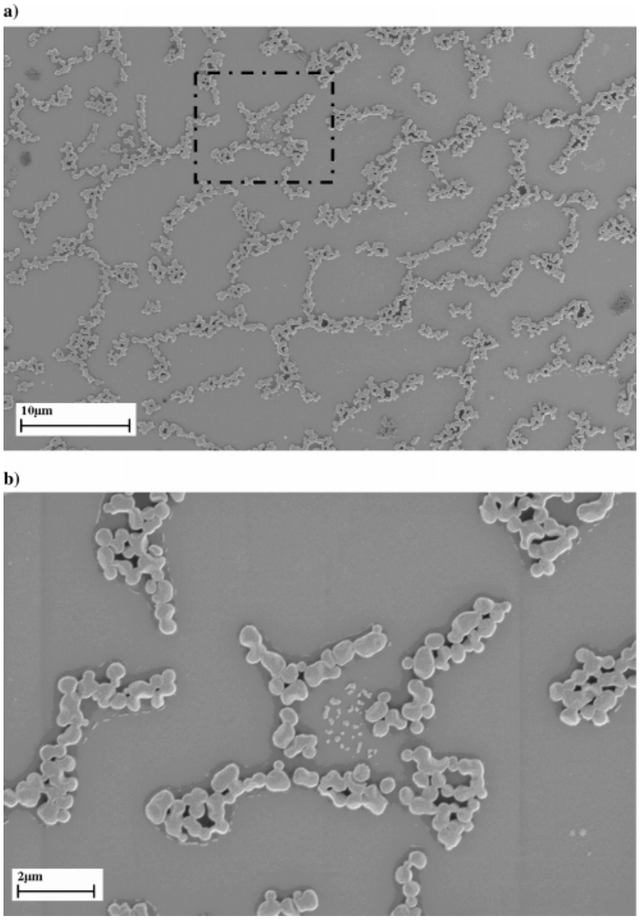

Figure 10. SEM images of polymer **PSDPQ** in its protonated form obtained from a 0.1 wt % THF solution. The area in the dashed square of a is given in enlargement in b. The bars in the images correspond to 10 and 2 μm, respectively.

Acknowledgment. The authors would like to thank Konarka Technologies Inc., Lowell, MA, for financial support. We are also grateful to Vasilis Drakopoulos (FORTH−ICE/HT) for his assistance in obtaining the AFM and SEM images and Sheila Rodman (Polaroid, Woltham, MA) for fruitful conversations.

CM047909R